Spatiotemporal formulation of the Kuramoto-Sivashinsky equation

Matthew N. Gudorf

January 10, 2019

Abstract

Turbulence is one of the oldest unsolved problems of classical physics. The study of turbulence is intimately tied to the study of chaotic partial differential equations, a discipline which has made significant advances as computing power has become more readily available. A number of these advances are the result of combining numerical simulations with older theories; for instance, in the study of fluid dynamics, numerical simulations paired with periodic orbit theory and dynamical systems theory have over the past two decades contributed greatly to the understanding of turbulent and chaotic behavior. The next logical step of extending these methods to systems with larger physical scales has proved to be very challenging. To address these challenges, this work offers a new spatiotemporal formulation to provide a new perspective which can possibly circumvent these difficulties. The main goal of this reformulation is to provide a qualitative and quantitative description of the infinite space-time behavior of the Kuramoto-Sivashinsky equation. [1]

[1] 2019-01-14 Predrag: basically, the rule is never any references in the abstract

1 Introduction

1.1 Literature review

Nonlinear dynamics, chaotic partial differential equations, and other related disciplines greatly benefit from accessability to computing power. Solutions almost always need to be determined numerically, as the equations usually lack analytic solutions.

Some great advances were made by combining custom numerical codes with the ideas from periodic orbit theory and dynamical systems theory. Two commonly used codes for incompressible shear flows, `openpipeflow` [29] and `Channelflow` [11]. These libraries are used by many to study incompressible shear flows with either cylindrical pipe or plane-Couette geometry.

With these codes, periodic orbits and equilibria of the respective equations can be found numerically [26, 28]. The number and impact of the studies that utilize these computational codes is impressive to say the least; however, their returns are diminishing over time and the next step forward is not obvious. This difficulty and ambiguity is the motivating force behind this body of work.

This study will be dedicated to the Kuramoto-Sivashinsky equation, a partial differential equation (PDE) that describes reaction-diffusion phenomena. A common interpretation is that it models the velocity field of a circular laminar flame front, e.g. the flames of a bunsen burner. Previous studies of the Kuramoto-Sivashinsky equation have covered a wide range of topics, including but not limited to: the geometry of the Kuramoto-Sivashinsky equation 's state-space [7], its unstable recurrent patterns [17], the dimension of an inertial manifold [8], the existence and bifurcations of steady solutions [20, 9], families of solutions and bifurcation analysis [15], and continuous symmetry reduction [4].

Spatiotemporal methods are not a new idea, they have been used in studies of the complex Ginzburg-Landau equation [19, 18], binary fluid convection [16], and plane-Poiseuille flow [22]. A spatiotemporal approach has also been stated as a possible approach by Brown and Kevrekidis [2]. In addition to these examples, Wang *et al.* [27] not only use a spatiotemporal formulation to solve equations using Lagrange multipliers, but also claim that their method outperforms other conventional methods in terms of scalability.

The main purpose of this work is to develop a spatiotemporal theory which can discover quantitative information of the Kuramoto-Sivashinsky equation on an infinite spatiotemporal domain. The aforementioned studies [19, 18, 16, 22, 2] use spatiotemporal methods to find solutions, but revert back to conventional methods of analysis after solutions are found. The goal of this work is to develop a purely spatiotemporal theory with new and unique numerical methods and tools of analysis.

1.2 Problem statement

The nondimensionalized form of the spatiotemporal Kuramoto-Sivashinsky equation is defined by

$$u_t(x,t) + u_{xx}(x,t) + u_{xxxx}(x,t) + \frac{1}{2}(u(x,t)^2)_x = 0\,, \tag{1}$$

where $u(x,t)$ is a scalar field defined on a two dimensional spatiotemporal domain. The general behavior of this PDE can be crudely described by the following process: long-wavelength instabilities pump energy into the system, which is transferred to short-wavelength scales via nonlinear coupling. The energy is then dissipated by the "hyper"-diffusion (fourth derivative) term.

This body of work will begin with a proper definition of the "spatiotemporal formulation". The next step is to develop methods for finding spatiotemporal solutions and then generate a collection of said solutions. Once the solution space is believed to be adequately sampled, the search for a set of small spatiotemporal solutions ("tiles") begins. These tiles will serve as the building blocks for a two-dimensional spatiotemporal symbolic dynamics. After a sufficient set of tiles is found, the set of rules that determine the admissibility of solutions must be generated. The success of the spatiotemporal formulation can and should be measured on both computational and theoretical grounds, but the metrics for success have yet to be determined.

2 Spatiotemporal Kuramoto-Sivashinsky equation

The use of doubly periodic boundary conditions, $u(x,t) = u(x+L,t) = u(x,t+T) = u(x+L,t+T)$ for $x \in [0,L]$ and $t \in [0,T]$, is constant through this work. These boundary conditions motivate the use of a Fourier-Fourier basis (hereafter referred to as the spatiotemporal Fourier basis). The most common and important term used in the following discussion is "spatiotemporal invariant 2-torus". This term will refer to a solution to the Kuramoto-Sivashinsky equation that is a 2-torus in configuration space due to the doubly-periodic boundary conditions. A real valued spatiotemporal Fourier basis will be used such that the scalar velocity field $u(x,t)$ has the following expansion,

$$u(x,t) = \frac{1}{\sqrt{NM}} \sum_{n,m=0}^{N/2,M/2} \Big(\tilde{a}_{n,m}(\cos(q_m x)\cos(\omega_n t)) + \tilde{b}_{n,m}(\sin(q_m x)\cos(\omega_n t)) + \tilde{c}_{n,m}(\cos(q_m x)\sin(\omega_n t)) + \tilde{d}_{n,m}(\sin(q_m x)\sin(\omega_n t)) \Big) . \tag{2}$$

Let $\tilde{\mathbf{u}}$ be defined as the vector composed of all real valued spatiotemporal Fourier coefficients, which is assumed to be ordered in such a manner that the subseqeunt equations and definitions are logically consistent. Substituting the Fourier expansion into (1) yields a system of nonlinear algebraic equations,

$$(\mathcal{D}_t - \mathcal{D}_{xx} + \mathcal{D}_{xxxx})\tilde{\mathbf{u}} + \sum_{n',m'} \tilde{u}_{n-n',m-m'}\tilde{u}_{n,m} = 0 , \tag{3}$$

which depend explicitly on the spatiotemporal Fourier coefficients and implicitly on the scalar parameters (T,L) through the spectral differentiation operators D_i. For numerical accuracy and simplicity, a *pseudospectral* formulation of (3) is used,

$$(\mathcal{D}_t - \mathcal{D}_{xx} + \mathcal{D}_{xxxx})\tilde{\mathbf{u}} + \frac{1}{2}\mathcal{D}_x\mathcal{F}(\mathcal{F}^{-1}(\tilde{\mathbf{u}})^2) = 0 . \tag{4}$$

The term "pseudospectral" refers to the specific manner in which the nonlinear term is calculated. The operators in (4), $\mathcal{F}$ and $\mathcal{F}^{-1}$, represent the forward and backwards Fourier transforms, respectively.

2.1 Spatiotemporal symmetries

The Kuramoto-Sivashinsky equation is equivariant under Galilean symmetry transformations, O(2) symmetry transformations in space, and SO(2) symmetry transformations in time.

Galilean transformations are defined by $u(x,t) \to u(x - vt, t) - v$, where v is an independent variable. This is the easiest symmetry to account for, which is done by enforcing the following constraint for all solutions,

$$\int u(t)\,\mathrm{d}x = 0 \quad \forall t \in [0,T] ,$$

which equates to constraining all spatiotemporal Fourier modes with spatial index $m = 0$ to zero. This constraint removes Galilean invariance from all further discussion; therefore, the focus shifts to symmetries that can be represented by subgroups of the spatiotemporal symmetry group, $\mathrm{O}(2) \rtimes \mathrm{SO}(2)$.

2.1.1 Discrete symmetries

Borrowing intuition from previous analysis of the Kuramoto-Sivashinsky equation, this formulation will consider only two discrete symmetries, spatial reflection symmetry and shift-reflection (spatial reflection and half-cell time translation) symmetry [4, 17]. For mathematical brevity, let R_x and $R_x\tau_{1/2}$ denote spatial reflection and shift-reflection operations, respectively. The action of spatial reflection is written,

$$R_x u(x,t) = -u(-x,t) \tag{5}$$

and shift-reflection operation is written,

$$R_x\tau_{1/2} u(x,t) = -u(-x, t+\frac{T}{2}) \tag{6}$$

Solutions that display these symmetries satisfy the corresponding invariance conditions,

$$R_x u(x,t) - u(x,t) = 0\,, \tag{7}$$

$$R_x\tau_t u(x,t) - u(x,t) = 0\,. \tag{8}$$

When the real valued spatiotemporal Fourier basis expansion (2) is substituted into (7) and (8), a set of conditions or "selection rules" that constrain the spatiotemporal Fourier coefficients is produced. These selection rules can also be interpreted as definitions for *symmetry invariant subspaces*. Reflection invariance implies antisymmetric parity in space; therefore all spatially symmetric modes are forced to be zero. Stated explicitly, reflection invariance implies,

$$\tilde{a}_{n,m}, \tilde{b}_{n,m} = 0\,, \tag{9}$$

Similarly, for shift-reflection symmetry, the spatially symmetric modes must be antisymmetric in time, while spatially antisymmetric modes must be symmetric in time (the time parity is with respect to $t = T/2$). Therefore the selection rules are given by,

$$\begin{aligned} \tilde{a}_{n,m}, \tilde{b}_{n,m} &= 0 \text{ for } n \text{ even and } m = 0 \\ \tilde{c}_{n,m}, \tilde{d}_{n,m} &= 0 \text{ for } n \text{ odd and } m = 0 \end{aligned} \tag{10}$$

It should be noted that shift-reflection symmetry is prevalent in fluid dynamics calculations [12, 13, 14, 24], it has not been discussed for either the spatiotemporal Kuramoto-Sivashinsky equation nor other spatiotemporal problems. In fact, the term "spatiotemporal symmetry" has not personally been observed in the literature.

2.1.2 Continuous spatial translation symmetry

The last remaining symmetry to be considered in this formulation is continuous spatial translation symmetry. This manifests in spatiotemporal invariant 2-torus solutions as a periodicity condition which depends on both the period of the solution T and spatial shift idiosyncratic to the solution, denoted by $g(\sigma) \in \mathrm{SO}(2)$,

$$u(x,t) = g \circ u(x, t + T_p) \tag{11}$$

σ denotes the idiosyncratic spatial translation ("the shift") of a solution. Two possible methods to deal with this continuous symmetry are: quotienting the symmetry via first Fourier mode slice [4, 3] or performing a coordinate transformation that maps the spatiotemporal field into a reference frame in which it is periodic, called the "mean-velocity frame". The difficulty of the spatiotemporal implementation of the slicing method is sufficient enough to warrant use of the mean-velocity frame method.

The mean-velocity frame is mathematically equivalent to using the ansatz (written in complex representation for brevity),

$$a_m(t) = e^{-\frac{2\pi i m \sigma t}{LT}} \sum_{n,m} \tilde{u}_{m,n} e^{\mathrm{i}(q_m x + \omega_n t)} \,. \tag{12}$$

This ansatz results in a modified equation due to the time derivative of the exponential prefactor,

$$(\mathcal{D}_t - \mathcal{D}_{xx} + \mathcal{D}_{xxxx} + \mathcal{S})\tilde{\mathbf{u}} + \frac{1}{2}\mathcal{D}_x \mathcal{F}(\mathcal{F}^{-1}(\tilde{\mathbf{u}})^2) = 0 \,. \tag{13}$$

This ansatz and subsequent equation modification are sufficient to find invariant 2-tori with spatial translation symmetry. In contrast to discrete symmetries, there are no selection rules defined by this symmetry. Now that all considered symmetries and their subsequent equations have been derived the next step is to develop numerical methods to solve said equations.

3 Numerical methods

This section derives and describes the various numerical methods and algorithms used to find invariant 2-torus solutions of the Kuramoto-Sivashinsky equation. While this is the lion's share of the work, specific details will be avoided as much as possible.

The structure of this section is as follows: first, initial condition generation is described in sect. 3.2. Second, a powerful yet sometimes prohibitively expensive method called the "damped Gauss-Newton" method (dGN) is described first in sect. 3.3. Finally, two faster but less powerful methods (in terms of rate of convergence) are derived. These are the "adjoint descent method" [10] and GMRES or "general minimized residual method" [21], which are described in sect. 3.4 and sect. 3.5, respectively.

3.1 Notation

First, let us define some notation that will be convenient for the following discussion. The *state space vector* $\mathbf{u}$ denotes a vector that contains all computational variables: the spatiotemporal Fourier modes, the period, spatial domain size, and the SO(2) parameter σ.

$$\mathbf{u} = (\tilde{\mathbf{u}}, T, L, \sigma) \tag{14}$$

The parameter σ is only present when the *a priori* assumption of continuous symmetry is made. Likewise, if we decide to keep either L or T fixed then the respective variable would no longer be present in $\mathbf{u}$.

If the Kuramoto-Sivashinsky equation is represented as a vector function $\mathbf{F}$, then the root-finding problem can be trivially rewritten as,

$$\mathbf{F}(\mathbf{u}) = \mathbf{0}\,, \tag{15}$$

A useful mathematical construction is the so-called *cost function*, written,

$$I(\mathbf{u}) = \frac{1}{2}||\mathbf{F}(\mathbf{u})||^2\,, \tag{16}$$

where the norm is the L_2 norm. The cost function is a non-negative scalar function that only equals zero when $\mathbf{F}(\mathbf{u}) = 0$. Therefore, solving $\mathbf{F} = \mathbf{0}$ is equivalent to solving for $I = 0$.

Last is the derivation of the equations used in the damped Gauss-Newton method, Let $\mathbf{u}* = \mathbf{u} + \delta\mathbf{u}$ be a root of $\mathbf{F}(\mathbf{u})$ such that $\mathbf{F}(\mathbf{u}^*) = 0$, then,

$$\begin{aligned}
\mathbf{F}(\mathbf{u}+\delta\mathbf{u}) &\approx \mathbf{F}(\mathbf{u}) + \frac{\partial \mathbf{F}}{\partial \mathbf{u}}(\delta\mathbf{u}) \\
\mathbf{F}(\mathbf{u}^*) &\approx \mathbf{F}(\mathbf{u}) + \frac{\partial \mathbf{F}}{\partial \mathbf{u}}(\delta\mathbf{u}) \\
0 &\approx \mathbf{F}(\mathbf{u}) + \frac{\partial \mathbf{F}}{\partial \mathbf{u}}\delta\mathbf{u} \\
-\mathbf{F}(\mathbf{u}) &\approx \frac{\partial \mathbf{F}}{\partial \mathbf{u}}\delta\mathbf{u}\,.
\end{aligned} \tag{17}$$

The last equation in (17) will be referred to as the "Newton equation". The matrix $\frac{\partial \mathbf{F}}{\partial \mathbf{u}}$ will be called the "Jacobian matrix" and denoted by J.

3.2 Initial condition generation

Initial condition generation is often overlooked as a place for improvement due to lack of possible methods. The algorithm described in this section is only afforded to a spatiotemporal formulation and has many computational advantages over the conventional "close recurrence" procedure for producing initial conditions used in refs. [6, 23].

Typically, the close recurrence method is comprised of storing a time-integrated series of points. Once the time integration finishes, the pointwise L_2 norm between different time series points are calculated. The minima of this pointwise calculation are taken to indicate trajectory segments that nearly close on themselves which approximate periodic orbits. The main disadvantage is that the computational cost increases substantially in the limit of large spatial domains.

The spatiotemporal initial condition generation method initializes an entire spatiotemporal domain at once by randomly assigning values to the real valued Fourier mode coefficients. After the computational modes are initialized, spatial and temporal scales are imposed via manipulation of the spectrum of Fourier modes. This procedure guarantees that the initial condition not only has the desired scales but is also doubly periodic and smooth. Some example initial conditions are displayed in figure 1.

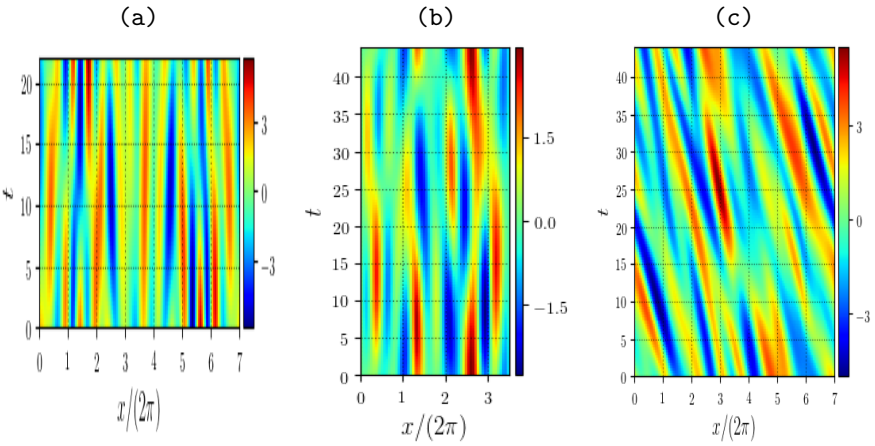

Figure 1: Example spatiotemporal initial conditions for three symmetry types, (a) shift-reflection, (b) reflection, (c) spatial translation.

3.3 Damped Gauss-Newton method

The first numerical method falls under the broad category of "Newton methods". This method directly solves the nonlinear root finding problem $\mathbf{F}(\mathbf{u}) = 0$ associated with the Newton equation,

$$\left[\frac{\partial \mathbf{F}}{\partial \tilde{\mathbf{u}}} \quad \frac{\partial \mathbf{F}}{\partial T} \quad \frac{\partial \mathbf{F}}{\partial L} \quad \frac{\partial \mathbf{F}}{\partial \sigma}\right] \delta\mathbf{u} = -\mathbf{F}(\mathbf{u})\,. \tag{18}$$

The Newton equation (18) is an over-determined (rectangular) system of equations. This requires us to either provide constraints to make the system square, or solve the system in a least squares manner. We elect to solve the least-squares problem, using what we call the "damped Gauss-Newton" method (dGN). "Gauss-Newton" implies that (18) is solved directly by calculating the Moore-Penrose pseudoinverse of the linear system, $A^+ \equiv (A^\top A)^{-1}A^\top$, such that the solution is given by $\delta x = A^+(-\mathbf{F}(\mathbf{u}))$.

The qualifier "damping" denotes the introduction of a scalar parameter d that is decreased until $I(\mathbf{u} + d(\delta\mathbf{u})) < I(\mathbf{u})$, is satisfied. A minimum bound ϵ is introduced such that $\epsilon < d < 1$. This ensures the norm of the solution does not become too small. In practice, for each solve of the Newton equation, $d_0 = 1$ and is divided by 2 until $I(\mathbf{u} + \frac{1}{2^k}(\delta\mathbf{u})) < I(\mathbf{u})$ or until $k = 10$.

3.4 Adjoint descent method

The previous section discussed a direct method for solving the Newton equation. While powerful, the matrix J must be explicitly formed so that the pseudoinverse can be calculated. This becomes expensive, sometimes prohibitively so, as the dimension of the state vector approaches $\dim[\mathbf{u}] \approx \mathcal{O}(10^4)$. Therefore, numerical methods that do not rely on explicit matrix construction are required. The first such method to be discussed is called the "adjoint descent method" [10].

The derivation of the adjoint descent method begins by taking a derivative of the cost function (16) with respect to a continuous fictitious time, denoted by τ. τ is a continuous variable which parameterizes the numerical method such that as $\tau \to \infty$, the cost function converges to zero $I(\tau) \to 0$.

$$\partial_\tau I(\mathbf{u}) = J^\top F \, \partial_\tau \mathbf{u} \,, \tag{19}$$

Eq. (19) includes an implicit choice for $\partial_\tau \mathbf{u}$. A useful choice is one that guarantees a monotonically decrease of the cost function. One specific choice,

$$\partial_\tau \mathbf{u} = -J^\top F \,, \tag{20}$$

will be referred to as the "adjoint direction". This choice ensures that the cost function is monotonically decreasing, as can be seen by,

$$\partial_\tau I(\mathbf{u}) = -||J^\top F||^2 \,, \tag{21}$$

where the right hand side is a strictly non-negative function. The adjoint descent method can be summarized simply as numerical integration in the adjoint descent direction.

3.5 GMRES

Yet another class of numerical methods implemented and utilized in this work are *iterative methods*. A very coarse description of iterative methods is that they are numerical methods that produce a sequence of approximate solutions x_k to linear system $Ax = b$ until some required tolerance or accuracy is achieved.

A common iterative method that is used for nonsymmetric matrices is known as GMRES [21]. GMRES falls under the broad category of Krylov subspace methods and has previously been used to find time invariant solutions in fluid dynamics [25, 5]. GMRES is comprised of two primary subroutines: Arnoldi iteration and a least-squares problem constrained to a Krylov subspace. Arnoldi iteration produces a Krylov subspace by successive matrix multiplication and orthonormalization via modified Graham-Schmidt method. The original optimization problem $||Ax - b|| = 0$ combined with the Arnoldi iteration recurrence relation,

$$AQ_k = Q_{k+1} H_k \,. \tag{22}$$

leads to the GMRES equation,

$$\begin{aligned} ||Ax - b|| &= ||AQ_k y - b|| \\ &= ||Q_{k+1} H_k y - b|| \\ &= ||H_k y - Q_{k+1}^T b|| \\ &= ||H_k y - \beta e_1|| \quad \text{where,} \\ \beta &= ||b|| \,, \end{aligned} \tag{23}$$

where e_1 is the unit vector whose first element is 1, and is of dimension $k+1$. The "GMRES solution" y, is a vector that minimizes the norm of $||H_k y - \beta e_1||$.

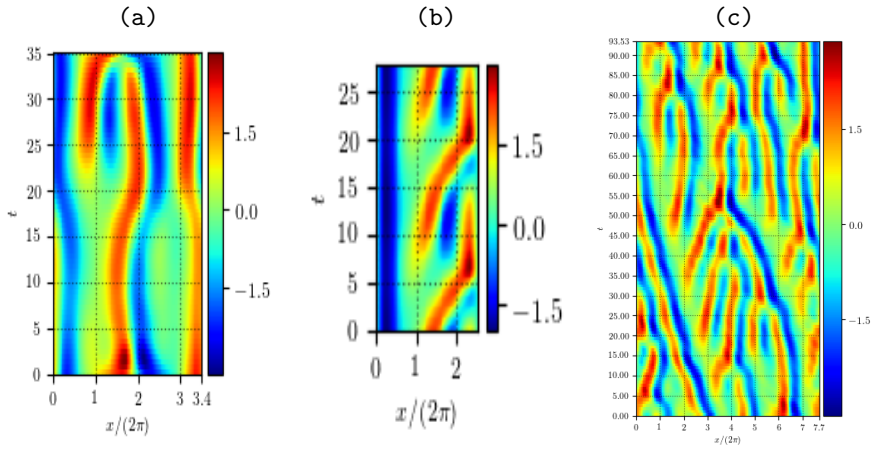

Figure 2: Examples of converged spatiotemporal solutions, the initial conditions used are the spatiotemporal scalar fields from figure 1. They have symmetries, (a) shift-reflection, (b) reflection, (c) spatial translation.

4 Current results

The numerical methods previously described are combined to create hybrid methods to find new spatiotemporal invariant 2-torus solutions to the Kuramoto-Sivashinsky equation. The most common and effective combination for finding solutions from experience is the combination of adjoint descent from sect. 3.4 with the damped Gauss-Newton method of sect. 3.3.

4.1 Collection of new solutions

A relatively large ($\mathcal{O}(10^3)$) number of new invariant 2-torus solutions have been found. Figure 2 displays the solutions that the example initial conditions, displayed in figure 1, converge to. This convergence proves that the spatiotemporal initial condition generation method from sect. 3.2 is indeed viable.

4.2 Spatiotemporal symbolic dynamics and tiling

One goal of this work is to develop a spatiotemporal symbolic dynamics but this is only worthwhile if the symbolic dynamics is simple enough to be useful. The term " spatiotemporal tile", or just "tile" is used to describe spatiotemporal solutions that are believed to be members of the spatiotemporal symbolic dynamic alphabet. The name "tile" was chosen to appeal to the intuition on how tiles are combined. The simplicity of the symbolic dynamics would be determined by the number of unique tile solutions as well as the set of rules that determine admissible symbolic combinations.

The new collection of converged solutions described in sect. 4.1 is assumed to adequately sample the overall space of solutions such that all spatiotemporal tiles can be found within. Patterns that appear frequently within the collection of solutions are likely candidates for spatiotemporal tiles. With this in mind, a collection of guess tiles was produced by manually scanning the database of new solutions by eye and picking out the most common patterns. These guesses are displayed in figure 3.

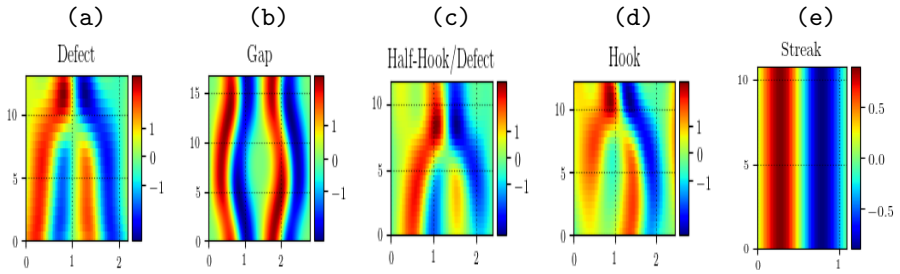

Figure 3: Guess "tiles" which were named: (a) defect,(b) gap,(c) half-defect,(d) hook,(e) streak.

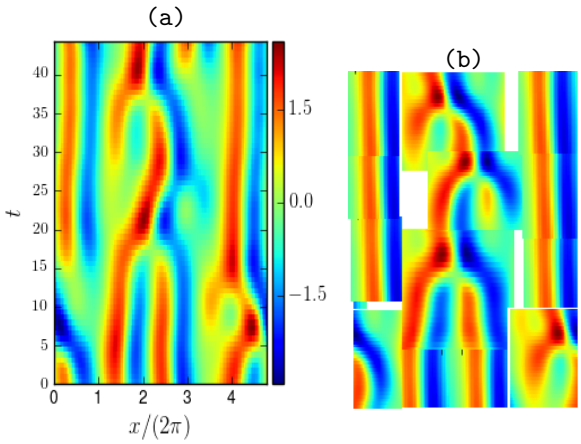

Figure 4: Qualitative example of how one might build larger spatiotemporal solutions from a library of small solutions. (a) A converged invariant 2-torus solution with shift-reflect symmetry; (b) An image thrown together using only a few subdomains that attempts to capture the behavior of (a).

To qualitatively demonstrate the purpose of the spatiotemporal tiles, the set of images from figure 3 was used to very crudely approximate a known spatiotemporal solution. This was mainly a test to see if the set of tiles in figure 3 was sufficiently large enough; if a pattern was missing from our collection it would imply we need to search more thoroughly. The approximation produced by cutting and pasting the images of guess tiles from figure 3 and the "target solution" are compared in figure 4. The approximation was constructed using only three images.

The four tile guesses that converged numerically are displayed in figure 5. Of these four spatiotemporal tiles, three were determined to be unique. The reduction from four to three tiles was the result of a comparison of the "defect" and "hook" tiles. Numerical continuation was used to match the domain sizes of the two tiles, after which the translational symmetries were quotiented to ensure that they were indeed the same solution. Visual comparison of the solutions displayed in figure 6 seems sufficient enough to claim that the two tiles are indeed identical.

The ability to numerically continue spatiotemporal tiles indicates that the tiles exist in continuous families. Alternatively, tiles exist on deformable spatiotemporal domains, determined by the parameters, T, L as opposed to static, rigid domains. These families actually offer a useful explanation for the overlooked fact that continuous families of spa-

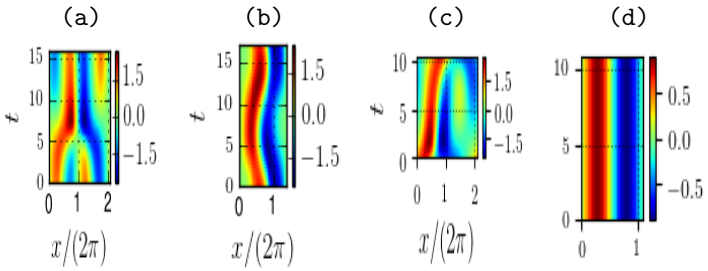

Figure 5: Numerically converged spatiotemporal tiles: (a)defect, (b)gap, (c)hook, (d)streak.

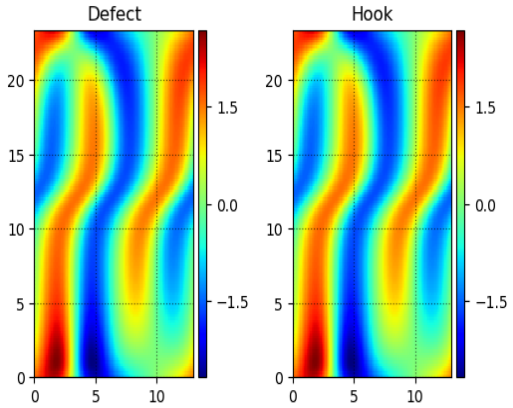

Figure 6: Spatiotemporal tiles: (left) "defect" tile, (right) "hook" tile. The tiles have been numerically continued to the same domain size $\tilde{L} \approx 2.06$. Spatial and temporal translational symmetries have been quotiented via first Fourier mode slice [4] for spatial translations and phase fixing for time translations.

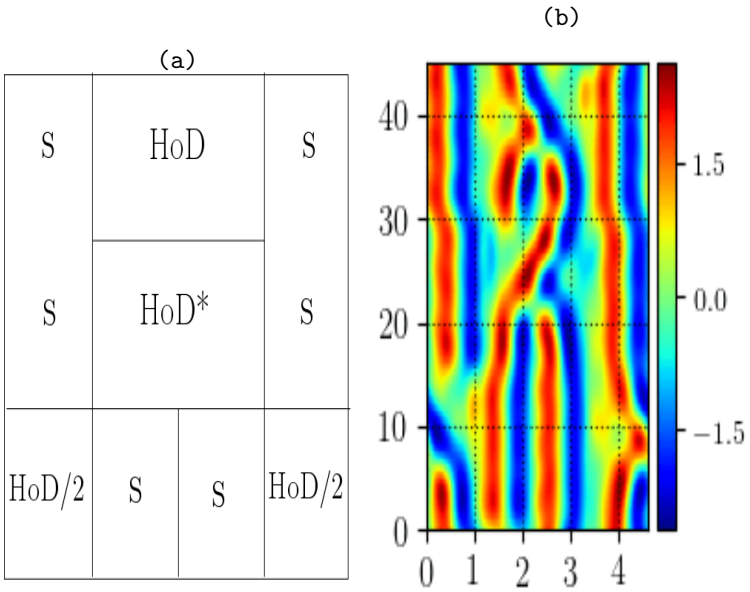

Figure 7: Initial condition attempting to reconstruct a known solution. The initial condition is displayed in both (a) spatiotemporal symbolic dynamical representation and (b)spatiotemporal scalar field representation. This initial condition converged but not to the desired solution

tiotemporal invariant 2-tori exist. The proposed reconciliation between symbolic dynamics and continuous families of solutions is that solutions each have a unique and constant symbolic representation but the deformability of the tiles allows solutions to exist as continuous families. One foreseeable problem;however, is that if the admissibility of tile combinations depends on the tiles' parameter values, the grammar might be hopelessly complex.

Acquiring a set of tiles is in and of itself not very useful, their utility is dependent on their ability to construct larger spatiotemporal solutions. As a proof of concept, the qualitative tiling displayed in figure 4 is now quantitatively constructed and converged numerically. Visual inspection was used to determine the specific tiles and subdomains used to construct the initial conditions. The symbolic representation and spatiotemporal scalar fields of the two initial conditions are displayed in figure 7 and figure 8 Both of these initial conditions converged numerically to different spatiotemporal invariant 2-tori. The second attempt is believed to be identical to the targeted solution (up to small time translation). All three numerically converged solutions are displayed in figure 9.

4.3 Spatiotemporal gluing

It was shown in figure 9 that an approximate spatiotemporal symbolic dynamics can be used to reconstruct known spatiotemporal invariant 2-torus solutions. The reconstruction process entailed creating combining approximate tiles together to form a larger spatiotemporal solution; there is no reason why this concept cannot extend to larger spatiotemporal invariant 2-tori. In other words, it should be possible to find large spatiotemporal invariant 2-torus solutions by combining smaller spatiotemporal invariant 2-tori together. While identical to the concept of combining tiles, this process will be referred to as "gluing" when combining two relatively large spatiotemporal invariant 2-tori. In figure 10 two spatiotem-

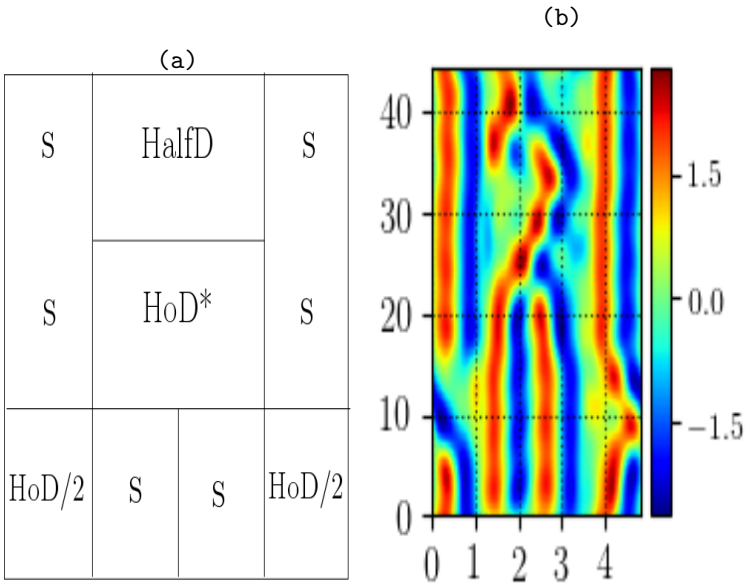

Figure 8: Initial condition attempting to reconstruct a known solution. The initial condition is displayed in both (a) spatiotemporal symbolic dynamical representation and (b)spatiotemporal scalar field representation. This initial condition converged to the desired solution

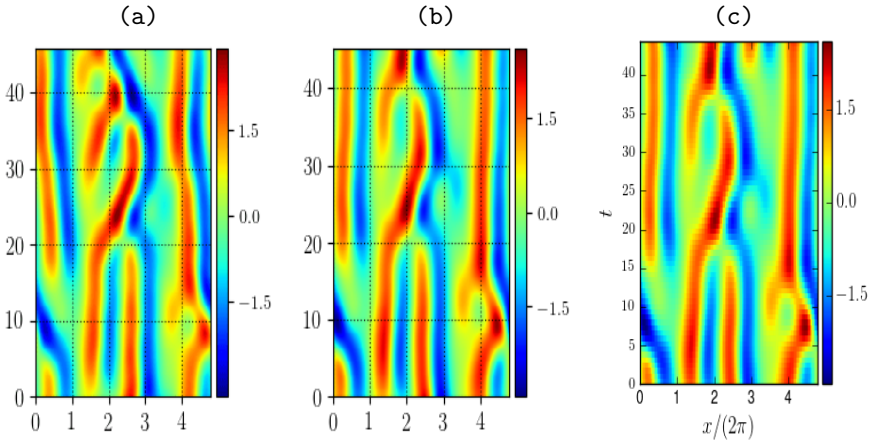

Figure 9: (a)Numerically converged spatiotemporal invariant 2-torus attained by numerically converging the initial condition (a) from figure 7. (b)Numerically converged spatiotemporal invariant 2-torus attained by numerically converging the initial condition (c) from figure 8. (c)Targeted solution. By visual inspection the converged solution (b) is equivalent to (c).

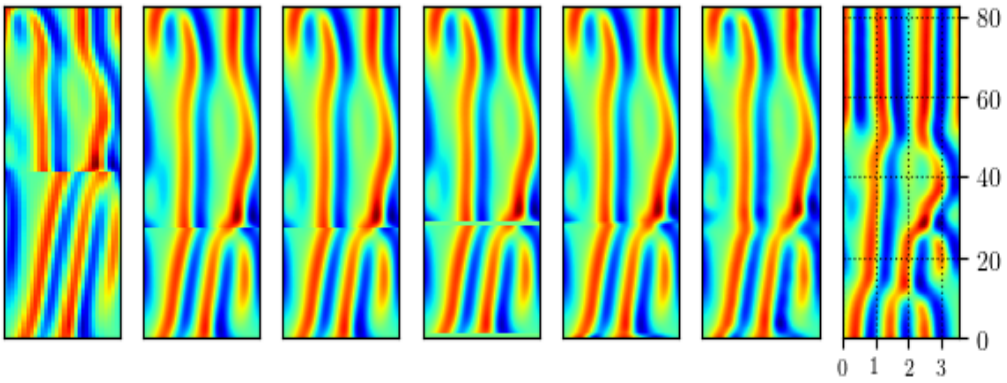

Figure 10: Schematic demonstration of the "gluing" of two invariant 2-torus solutions with spatial translation symmetry with figures. From left to right, the figures represent, (1) the original spatiotemporal fields combined vertically, (2) fields with correct aspect ratio, (3) rotated fields that minimize boundary differences, (4) fields with zero padding, (5) fields with convex buffers, (6) field with truncated spatiotemporal modes, (7) numerically converged solution.

poral invariant 2-tori with continuous spatial translation symmetry are glued temporally and numerically converged. Likewise, in figure 11 two spatiotemporal invariant 2-tori with shift-reflection symmetry have been spatially glued and numerically converged.

The specific steps of the gluing process depend on the symmetry of the initial invariant 2-tori; currently, invariant 2-tori that are being glued together always have the same symmetry, and the gluing is performed in a symmetry preserving manner. The process can be summarized by the following numbered list.

1. Choose two spatiotemporal invariant 2-torus solutions to combine
2. Choose whether to glue spatially or temporally
3. Increase the resolution of the initial conditions by interpolation
4. Modify the discretizations to enforce the correct aspect ratio
5. (If symmetry is continuous) Rotate the two initial spatiotemporal fields to minimize the difference at the gluing boundaries, ensure fields have spatial shifts with the same sign by applying spatial reflection
6. (If symmetry is discrete) Test various combinations of fundamental domains and choose the best combination as determined by cost function residual
7. Create zero-padding regions between the boundaries
8. Fill in the zero-padding with convex combinations of the scalar field boundaries
9. Rediscretize the final spatiotemporal field to reduce the number of computational variables

The importance of this method is that it constitutes an alternative method for finding solutions on larger spatial domains for this equation as well as others; three dimensional fluid dynamics problems, for example.

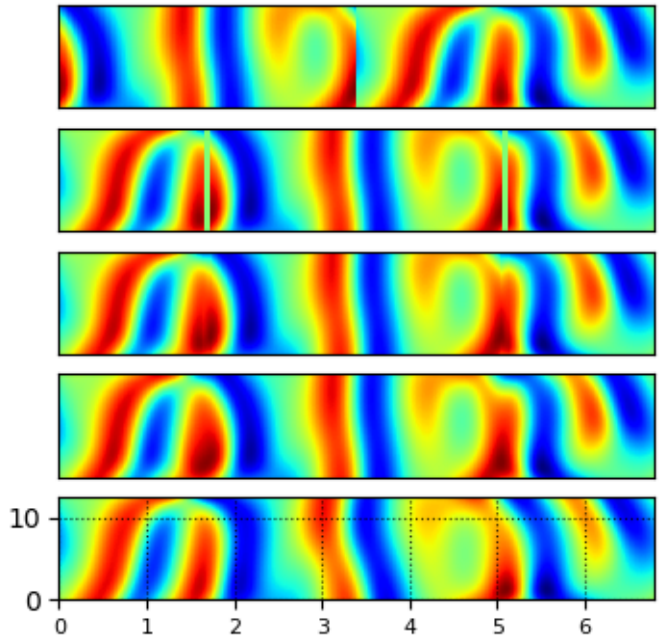

Figure 11: Schematic demonstration of spatially "gluing" two invariant 2-torus solutions with shift-reflection symmetry. From top to bottom, the figures represent, (1) the original spatiotemporal fields side-by-side, (2) fields with zero padding, (3) fields with zero padding filled in with convex combinations of boundaries, (4) field with truncated spatiotemporal modes, (5) numerically converged solution.

4.4 Summary of current results

The currents results of this work include methods that find invariant 2-tori tile invariant 2-tori and glue invariant 2-tori demonstrate the computational usefulness of spatiotemporal methods. The spatiotemporal theory, however, is currently composed of claims and assertions that appeal to intuition. Hopefully, old theoretical machinery and new discoveries will advance the theory to a place where rigorous and quantitative claims can be made and proved; especially in the infinite space-time limit. One of the main accomplishments is the ability to find invariant 2-tori defined on relatively large spatial domains with no a priori knowledge other than the equations and the symmetry of the solution.

5 Future work

5.1 Spatiotemporal symbolic dynamics

The next major step of this project is to complete the alphabet and grammar of the spatiotemporal symbolic dynamics of the Kuramoto-Sivashinsky equation , if possible. In other words, the goal is to discover all continuous families of tiles as well as the rules that govern the admissibility of tile combinations. Finding a minimal set of tiles seems possible; there is a lower bound on domain size $\tilde{L} = \frac{L}{2\pi} = 1$ below which the laminar solution $u = 0$ is a global attractor [17]. As L increases, unstable solutions are born from sequences of bifurcations [15, 1]. It is unknown whether there exists an upper bound for the spatial domain size of tile solutions, but it does not seem unreasonable to conjecture that patterns start to repeat after the domain size exceeds the largest spatial correlation length. The less reasonable goal seems to be enumerating the grammar of the symbolic dynamics that determines admissible patterns. All hope is not lost, however, as the grammar might be able to be procedurally generated with a complete set of tiles. The procedure would consist of attempting to numerically converge initial conditions built from all symbolic combinations of tiles. If the combination is not found then the corresponding spatiotemporal symbol shape would be inadmissible. If every invariant 2-torus can be decomposed into a collection of tiles then quantitative behavior on infinite spatiotemporal domains would only depend on the frequency of spatiotemporal tiles as opposed to the frequency of arbitrarily large spatiotemporal invariant 2-torus solutions.

5.2 Quasi 2D Kolmogorov flow

In an effort to increase the impact of the techniques developed here we intend to apply the same numerical methods on a more computationally challenging system; the quasi (depth averaged) 2-D Kolmogorov flow with periodic boundary conditions [5]. This work will be performed concurrently with the Kuramoto-Sivashinsky equation research. Essentially, the generalization of the spatiotemporal formulation will be tested. This is an intermediate step between the spatiotemporal Kuramoto-Sivashinsky equation and three dimensional fluid flows. It is currently unknown whether it will be computationally viable without first finding even better numerical methods because of the even greater number of computational variables.

References

[1] D. Armbruster, J. Guckenheimer, and P. Holmes. Kuramoto-Sivashinsky dynamics on the center-unstable manifold. *SIAM J. Appl. Math.*, 49:676–691, 1989.

[2] H. S. Brown and I. G. Kevrekidis. Modulated traveling waves for the Kuramoto-Sivashinsky equation. In D. Benest and C. Froeschlé, editors, *Pattern Formation: Symmetry Methods and Applications*, pages 45–66. AMS, Providence, RI, 1996.

[3] N. B. Budanur and P. Cvitanović. Unstable manifolds of relative periodic orbits in the symmetry-reduced state space of the Kuramoto-Sivashinsky system. *J. Stat. Phys.*, 167:636–655, 2015.

[4] N. B. Budanur, P. Cvitanović, R. L. Davidchack, and E. Siminos. Reduction of the SO(2) symmetry for spatially extended dynamical systems. *Phys. Rev. Lett.*, 114:084102, 2015.

[5] G. Chandler and R. Kerswell. Simple invariant solutions embedded in 2D kolmogorov turbulence. *J. Fluid. Mech.*, 722:554–595, 2013.

[6] G. J. Chandler and R. R. Kerswell. Invariant recurrent solutions embedded in a turbulent two-dimensional Kolmogorov flow. *J. Fluid Mech.*, 722:554–595, 2013.

[7] P. Cvitanović, R. L. Davidchack, and E. Siminos. On the state space geometry of the Kuramoto-Sivashinsky flow in a periodic domain. *SIAM J. Appl. Dyn. Syst.*, 9:1–33, 2010.

[8] X. Ding, H. Chaté, P. Cvitanović, E. Siminos, and K. A. Takeuchi. Estimating the dimension of the inertial manifold from unstable periodic orbits. *Phys. Rev. Lett.*, 117:024101, 2016.

[9] C. Dong and Y. Lan. Organization of spatially periodic solutions of the steady Kuramoto-Sivashinsky equation. *Commun. Nonlinear Sci. Numer. Simul.*, 19:2140–2153, 2014.

[10] M. Farazmand. An adjoint-based approach for finding invariant solutions of Navier-Stokes equations. *J. Fluid M.*, 795:278–312, 2016.

[11] J. F. Gibson. Channelflow: A spectral Navier-Stokes simulator in C++. Technical report, U. New Hampshire, 2013. `Channelflow.org`.

[12] J. F. Gibson, J. Halcrow, and P. Cvitanović. Visualizing the geometry of state-space in plane Couette flow. *J. Fluid Mech.*, 611:107–130, 2008.

[13] J. F. Gibson, J. Halcrow, and P. Cvitanović. Equilibrium and traveling-wave solutions of plane Couette flow. *J. Fluid Mech.*, 638:243–266, 2009.

[14] G. Kawahara and S. Kida. Periodic motion embedded in plane Couette turbulence: Regeneration cycle and burst. *J. Fluid Mech.*, 449:291, 2001.

[15] I. G. Kevrekidis, B. Nicolaenko, and J. C. Scovel. Back in the saddle again: a computer assisted study of the Kuramoto-Sivashinsky equation. *SIAM J. Appl. Math.*, 50:760–790, 1990.

[16] E. Knobloch and D. R. Moore. Minimal model of binary fluid convection. *Phys. Rev. A*, 42:4693–4709, 1990.

[17] Y. Lan and P. Cvitanović. Unstable recurrent patterns in Kuramoto-Sivashinsky dynamics. *Phys. Rev. E*, 78:026208, 2008.

[18] V. López. Numerical continuation of invariant solutions of the complex Ginzburg–Landau equation, 2015.

[19] V. López, P. Boyland, M. T. Heath, and R. D. Moser. Relative periodic solutions of the complex Ginzburg-Landau equation. *SIAM J. Appl. Dyn. Syst.*, 4:1042–1075, 2006.

[20] D. Michelson. Steady solutions of the Kuramoto-Sivashinsky equation. *Physica D*, 19:89–111, 1986.

[21] Y. Saad and M. H. Schultz. GMRES: A generalized minimal residual algorithm for solving nonsymmetric linear systems. *SIAM J. Sci. Stat. Comput.*, 7:856–869, 1986.

[22] I. Soibelman and D. I. Meiron. Finite-amplitude bifurcations in plane Poiseuille flow: two-dimensional Hopf bifurcation. *J. Fluid Mech.*, 229:389, 1991.

[23] B. Suri, J. Tithof, R. O. Grigoriev, and M. F. Schatz. Unstable equilibria and invariant manifolds in quasi-two-dimensional Kolmogorov-like flow. *Phys. Rev. E*, 98:023105, 2018.

[24] D. Viswanath. Recurrent motions within plane Couette turbulence. *J. Fluid Mech.*, 580:339–358, 2007.

[25] D. Viswanath. The critical layer in pipe flow at high Reynolds number. *Philos. Trans. Royal Soc. A*, 367:561–576, 2009.

[26] F. Waleffe. Exact coherent structures in channel flow. *J. Fluid Mech.*, 435:93–102, 2001.

[27] Q. Wang, S. A. Gomez, P. J. Blonigan, A. L. Gregory, and E. Y. Qian. Towards scalable parallel-in-time turbulent flow simulations. *Phys. Fluids*, 25:110818, 2013.

[28] H. Wedin and R. R. Kerswell. Exact coherent structures in pipe flow. *J. Fluid Mech.*, 508:333–371, 2004.

[29] A. P. Willis. Openpipeflow: Pipe flow code for incompressible flow. Technical report, U. Sheffield, 2014. `Openpipeflow.org`.